Central Force of Baryon-Baryon Interactions with $S = -2$ in the SU_6 Quark Model

Choki NAKAMOTO, Yasuyuki SUZUKI* and Yoshikazu FUJIWARA**

Research Center for Nuclear Physics, Osaka University, Ibaraki 567
*Department of Physics, Niigata University, Niigata 950-21
***Department of Physics, Kyoto University, Kyoto 606-01*

A simultaneous description of the central interaction of the hyperon-nucleon and hyperon-hyperon systems with strangeness $S = -2$ is attempted by using the $(3q)$-$(3q)$ resonating-group formulation in the SU_6 quark model. The full Fermi-Breit qq interaction with explicit flavor symmetry breaking is supplemented by the effective meson-exchange potentials generated from the scalar-meson nonet and π and K mesons of the Nijmegen potential model-F. The central forces predicted by the quark-model potential have the flavor-dependent medium-range attraction in the $S = -2$ system just like in the $S = -1$ system. The strength of the ΞN-$\Lambda\Lambda$ transition potential in the ^1S channel strongly depends on the effect of the flavor symmetry breaking generated from the mass difference between ud and s quarks. The two-baryon system in the ^1S state of isospin 0 is predicted to have the binding energy of -19.25 MeV from the $\Lambda\Lambda$ threshold. The cross sections induced by the Ξ^-p reaction at $p_\Xi = 500$ MeV/c are predicted as follows: $\sigma_{el}(\Xi^-p) = 27.7$ mb, $\sigma(\Xi^-p \to \Xi^0 n) = 24.5$ mb, and $\sigma(\Xi^-p \to \Lambda\Lambda) = 15.4$ mb.

§1. Introduction

The study of the interaction between two octet-baryons in the strangeness $S = -2$ sector has recently been attracting much attention.[1]-[3] It is since Jaffe predicted the existence of the H-particle[4] that many authors have focussed on the $^1S_0$ interaction in the isospin $I = 0$ channel of $\Lambda\Lambda$, ΞN and $\Sigma\Sigma$ systems. The discovery of a double-Λ hypernucleus, which was observed in 1991 by the emulsion-counter hybrid technique[5], has also directed our attention to the $\Lambda\Lambda$ interaction. In spite of the technical difficulties in its measurement, a Ξ^-p scattering experiment through the (K^-, K^+) reaction is being planned to get information on the ΞN interaction as well as the transition potential to the $\Lambda\Lambda$ system.

The system with $S = -2$ comprising two octet-baryons includes the $\Lambda\Lambda$, ΞN, $\Sigma\Lambda$ and $\Sigma\Sigma$ channels. They have richer coupling features than in the case of $S = -1$ system. For example, the $\Lambda\Lambda$, ΞN and $\Sigma\Sigma$ channels couple each other in the state with $I = 0$, while the ΞN, $\Sigma\Lambda$ and $\Sigma\Sigma$ channels couple each other in the state with $I = 1$. For the correct evaluation of Ξ^-p scattering observables, one should therefore take into account the effect of transitions to these other channels.

Nijmegen group[6]-[8] and Jülich group[9] have extensively studied the baryon-baryon interaction in the $S = 0$ and -1 systems by using the one-boson exchange model. They have attempted a systematic description of the interaction by fixing the coupling constants between the octet baryons and the nonet mesons through the SU_3 relations and succeeded in obtaining reasonable reproduction of the low-energy
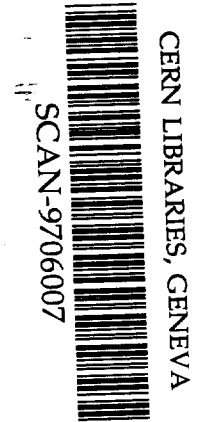
hyperon-nucleon (YN) data. The treatment of the short-range interaction is more or less phenomenological in both models: The hard core radius in Nijmegen model-D [6] and the cut-off mass in Jülich model are fixed to reproduce the scarce YN scattering data, whereas the hard core radius in Nijmegen model-F [7] and the cut-off mass in Nijmegen soft core model [8] are determined through relating the flavor SU_3 symmetry of the YN system to that of the nucleon-nucleon (NN) system in which rich data are available. When these models are extended to the $S = -2$ system, it is clear that the above prescription does not apply straightforwardly: In the former case there are no available experimental data on the $S = -2$ system, and in the latter case the $S = -2$ system contains a unique symmetry of flavor singlet which appears in neither of the $S = 0$ and -1 systems. The extension of these models to the $S = -2$ system, therefore, cannot be trivially made. It is desirable to acquire such a framework that describes the $S = 0$ and -1 systems consistently for a systematic study of the $S = -2$ system.

The quark cluster model inspired by the QCD attempts at describing the baryon-baryon interaction by including some phenomenological confinement potential and a one-gluon exchange qq potential (OGEP). In this model the short range part of the interaction is unambiguously determined by the quark-exchange kernel, once the parameters of the OGEP are fixed to reproduce the single-baryon properties. [10],[11] To describe the nuclear force realistically the model must be reinforced by the meson exchange effect which is essential in the medium and long range regions of the interaction. This framework has the advantage that it can straightforwardly be extended to any interaction among the octet baryons through the SU_3 Wigner coefficients. In fact some papers have already discussed the $S = -2$ system in the quark cluster model. Straub *et al.* [12] studied the low-energy YN cross section as well as the H-particle by incorporating the pseudoscalar- (PS-) meson nonet exchange at the quark level and the flavor singlet scalar- (S-) meson exchange at the baryon level. Koike, Shimizu and Yazaki [13] employed the flip-flop model for the confinement mechanism, and took into account the PS-meson octet exchange and the flavor singlet S-meson exchange with the form factor being introduced at the baryon level. Takeuchi and Oka [14] took into account the effects of instanton-induced interactions as well as a phenomenological medium-range attraction which is independent of spin and flavor. We have to note, however, that due care should be taken of how to introduce the effective meson-exchange potential (EMEP). For example, the usage of the flavor singlet S-meson is not appropriate to reproduce the correct flavor dependence of the nuclear force and to describe the NN, ΛN and ΣN interactions simultaneously. [15]

We have recently proposed a simultaneous description of the NN, ΛN and ΣN interactions [16]-[19] in the SU_6 quark model formulated in the resonating-group method (RGM). The full Fermi-Breit (FB) interaction with explicit flavor symmetry breaking (FSB) is incorporated in the calculation. The difference in introducing the EMEP has led to three models called RGM-F, [16],[17] FSS [18],[19] and RGM-H, [19] although in all of these the YN interaction is treated consistently with the NN interaction. The model RGM-F, which is the simplest among the three, introduces only the tensor component of the π- and K-meson exchanges besides the central

force of the S-meson nonet exchanges. In this model, we first calculate RGM kernels for pure flavor singlet mesons and then introduce the explicit flavor dependence of the Nijmegen model-F[7] potential for the products of the coupling constants. Other models called FSS and RGM-H introduce not only the tensor component generated from the π- and K-meson exchanges, but also the spin-spin and tensor components of the PS-meson nonet exchange. In FSS the spin-flavor factors of the quark-exchange RGM kernel are explicitly evaluated at the quark level, while in RGM-H the description similar to RGM-F are used only for the isoscalar S-meson exchange to get the overall reproduction of the YN cross sections. Although some difference is seen in these models for the coupling features of the ΛN-ΣN systems, RGM-F is the simplest which describes NN and YN data simultaneously. It is straightforward to extend these models worked out for the $S = 0$ and -1 systems to the $S = -2$ system through the SU_3 invariance of the baryon-meson coupling constants of the EMEP.

A theoretical study on the $\Xi^- p$ system is interesting itself and moreover urgently requested by experimentalists as a measurement will be performed in a near future. No theoretical prediction for the observables of the $\Xi^- p$ system, e.g., the scattering cross section, has so far been given systematically and realistically. Only the S-wave phase shift of the ΞN system was investigated in the above quark model.[12],[13] Since the ΞN system has the complexity of channel coupling with other channels, it will be legitimate to first understand the ΞN interaction in a single-channel approximation. The central force of the baryon-baryon interaction is an outcome of combined contributions from both of the quark kinematics and the meson-cloud effect, whereas the tensor force is generated mostly from the meson-exchange effect and the spin-orbit (LS) force is reasonably well accounted for in the quark model.[20] The understanding of the central force is essential to disentangle the complicated characteristics of the interaction.

The purpose of this paper is to investigate the behavior of the central force of various baryon-baryon systems with $S = -2$ in a single-channel approximation. We apply the simplest framework of RGM-F to the system with $S = -2$ and focus on the interaction in the S- and P-waves. The organization of this paper is as follows. In the next section the formulation of our model is briefly recapitulated together with the definition of the effective local potential. Characteristic features of the central force are discussed in §3 by considering the quark Pauli effect and the role of color-magnetic piece of the FB interaction. The RGM calculation of the phase shifts are also shown in this section. A preliminary result of the coupled channel calculation for the ΞN cross section and the binding energy of the H particle is also discussed in this section. In §4 our quark-model (QM) potential is compared with the Nijmegen potential. The last section is devoted to a brief summary.

§2. Recapitulation of the formulation

The detail of our framework is already given in Refs. 15) and 16). Here we only recapitulate the main part for the sake of convenience.

The single-baryon wave function ψ_B of three quarks is composed of three parts,

the symmetric orbital part $\phi^{(orb)}(123)$, the spin-flavor part $W^{[3]}_{\frac{1}{2}(11)a}(123)$, and the antisymmetric color part $C(123)$:

$$\psi_B(123) = \phi^{(orb)}(123)\, W^{[3]}_{\frac{1}{2}(11)a}(123)\, C(123) \ , \qquad (2\cdot1)$$

where [3] denotes the 3-particle symmetric state of the SU_6 spin-flavor wave function, the label $1/2(11)$ stands for the octet-baryon with spin $1/2$ and the flavor SU_3 symmetry of (11) in the Elliott notation. The SU_3 subgroup label a specifies a member of the octet-baryons. For $\phi^{(orb)}(123)$ we adopt a simple $(0s)^3$ configuration with a common harmonic-oscillator constant b. The center-of-mass (c.m.) motion is eliminated in $\phi^{(orb)}(123)$ with the use of the usual definition of the c.m. coordinate $X_G = (r_1 + r_2 + r_3)/3$. We thus assume that the orbital function for the $(3q)$ clusters is flavor independent and taken to be common in all the octet baryons.

The RGM wave function for the $(3q)$-$(3q)$ system with the inter baryon relative-motion function $\chi_\alpha(r)$ can be expressed as

$$\Psi = \sum_\alpha \mathcal{A}'\{\phi_\alpha \chi_\alpha(\boldsymbol{R})\} \ , \qquad (2\cdot2)$$

where $\mathcal{A}'$ denotes the antisymmetrization operator, and the channel wave function ϕ_α is defined through $\phi^{(orb)}(123)\,\phi^{(orb)}(456)\,\xi^{SF}_\alpha \xi^C$ with $\xi^C = C(123)\,C(456)$. A product of the two spin-flavor functions is given in the isospin-coupled basis ξ^{SF}_α, which is the eigenfunction of P^{SF}_0, the core-exchange operator of the two $(3q)$ clusters in the spin-flavor space. The operator defines the flavor symmetry phase $\mathcal{P}$ through

$$P^{SF}_0 \xi^{SF}_\alpha = (-1)^{1-S}\mathcal{P}\xi^{SF}_\alpha \ , \qquad (2\cdot3)$$

where the subscript α specifies a set of quantum numbers of the channel wave function, $\alpha = [1/2(11)a_1,\, 1/2(11)a_2]\, SS_zYII_z; \mathcal{P}$. Here S denotes the total spin, S_z its z component, Y the hypercharge, I the isospin and I_z its z component.

The QM Hamiltonian consists of the non-relativistic kinetic energy term, the quadratic confinement potential, the full FB interaction with explicit quark mass dependence, and the S-, π- and K-meson exchange potentials acting between quarks;

$$H = \sum_{i=1}^{6}\left(m_i c^2 + \frac{\boldsymbol{p}_i^2}{2m_i}\right)$$
$$+ \sum_{i<j=1}^{6}\left(U^{Cf}_{ij} + U^{FB}_{ij} + \sum_{\beta=\epsilon,S^*,\delta,\kappa} U^{S\beta}_{ij} + \sum_{\beta=\pi,K} U^{PS\beta}_{ij}\right) \ , \qquad (2\cdot4)$$

where m_i and $\boldsymbol{p}_i$ are the mass and the momentum operator of the i-th quark, respectively. Here $U^{Cf}_{ij} = -(\lambda^c_i \cdot \lambda^c_j)a_c r^2_{ij}$ with $r_{ij} = |r_{ij}| = |x_i - x_j|$ is the confinement potential of quadratic power law with a_c denoting the confining strength. The color SU_3 generator, λ^c_i, is normalized in such a way that the exchange operator P^C_{ij} in the color space is given by $(1/2)(\lambda^c_i \cdot \lambda^c_j) + 1/3$. The central component of the qq FB interaction, U^{FB}_{ij}, is composed of the color-Coulombic (CC) term,

$U_{ij}^{CC} = (1/4)\alpha_S \hbar c\,(\lambda_i^c \cdot \lambda_j^c)/r_{ij}$, the momentum-dependent retardation (MC) term,

$$U_{ij}^{MC} = -\frac{1}{4}\alpha_S \hbar c(\lambda_i^c \cdot \lambda_j^c)\frac{1}{2m_i m_j c^2}\left(\frac{\boldsymbol{p}_i \cdot \boldsymbol{p}_j}{r_{ij}} + \frac{\boldsymbol{r}_{ij} \cdot (\boldsymbol{r}_{ij} \cdot \boldsymbol{p}_i)\boldsymbol{p}_j}{r_{ij}^3}\right) \qquad (2\cdot5)$$

and the color-magnetic (GC) term,

$$U_{ij}^{GC} = -\frac{1}{4}\alpha_S \hbar c(\lambda_i^c \cdot \lambda_j^c)\frac{\pi\hbar^2}{2c^2}\left(\frac{1}{m_i^2} + \frac{1}{m_j^2} + \frac{4}{3m_i m_j}\boldsymbol{\sigma}_i \cdot \boldsymbol{\sigma}_j\right)\delta(\boldsymbol{r}_{ij}) \ . \qquad (2\cdot6)$$

Here α_S is the quark-gluon coupling constant and $\boldsymbol{\sigma}_i$ denotes the spin SU_2 generator. In Eq. (2·4), $U_{ij}^{S\beta}$ and $U_{ij}^{PS\beta}$ denote the central force generated from the S-meson nonet exchange and the tensor force generated from the π- and K-exchange, respectively. $U_{ij}^{S\beta}$ is expressed as follows;

$$U_{ij}^{S\beta} = -\sum_\beta g^2 m_\beta Y(m_\beta r_{ij}) \ , \qquad (2\cdot7)$$

where g denotes the quark-meson coupling constant, m_β the mass of the meson β and $Y(x)$ is the Yukawa function $Y(x) = e^{-x}/x$.

The RGM equation is derived from the variational principle, subject to the change of the relative wave function $\chi_\alpha(\boldsymbol{R})$ of Eq. (2·2) and reads as follows;

$$\left[\varepsilon_\alpha + \frac{\hbar^2}{2\mu_\alpha}\left(\frac{\partial}{\partial \boldsymbol{R}}\right)^2 - V_{\alpha D}^{CN}(\boldsymbol{R}) - V_{\alpha D}^{TN}(\boldsymbol{R})S_{12}\right]\chi_\alpha(\boldsymbol{R})$$
$$= \sum_{\alpha'}\int d\boldsymbol{R}' G_{\alpha\alpha'}(\boldsymbol{R}, \boldsymbol{R}')\chi_{\alpha'}(\boldsymbol{R}') \ , \qquad (2\cdot8)$$

where the relative energy ε_α is defined by subtracting the internal energies of the clusters in the channel α from the total energy, μ_α is the calculated reduced mass, and S_{12} denotes the tensor operator at the baryon level. Here the integral kernel $G_{\alpha\alpha'}(\boldsymbol{R}, \boldsymbol{R}')$ is defined through

$$G_{\alpha\alpha'}(\boldsymbol{R}, \boldsymbol{R}') = \sum_\Omega \mathcal{M}_{\alpha\alpha'}^{(\Omega)}(\boldsymbol{R}, \boldsymbol{R}') - \varepsilon_\alpha \mathcal{M}_{\alpha\alpha'}^N(\boldsymbol{R}, \boldsymbol{R}') \ , \qquad (2\cdot9)$$

where $\mathcal{M}_{\alpha\alpha'}^N(\boldsymbol{R}, \boldsymbol{R}')$ is the normalization exchange kernel and $\mathcal{M}_{\alpha\alpha'}^{(\Omega)}(\boldsymbol{R}, \boldsymbol{R}')$ is the exchange kernel corresponding to the interaction piece Ω. For the detailed definition of $\mathcal{M}_{\alpha\alpha'}^{(\Omega)}(\boldsymbol{R}, \boldsymbol{R}')$, see Ref. 15). The Hamiltonian of Eq. (2·4) includes the c.m. kinetic-energy and the Galilean non-invariant terms like the MC term. However, the existence of these terms does not pose any problem if the RGM kernels are evaluated in the c.m. system. [15] The direct potential $V_{\alpha D}^{CN}(\boldsymbol{R})$ of Eq. (2·8) are given by

$$V_{\alpha D}^{CN}(\boldsymbol{R}) = -9g^2 m_\beta Y_{\alpha_0}(m_\beta R) \ , \qquad (2\cdot10)$$

where $Y_{\alpha_0}(m_\beta R)$ with $\alpha_0 = (m_\beta b)^2/3$ is the modified Yukawa function with a Gaussian form factor $F(\boldsymbol{q}^2) = \exp\{-(b\boldsymbol{q})^2/6\}$ (see Eq. (A2) of Ref. 16)).

As is discussed in Ref. 15), it is essential to choose an appropriate flavor dependence for the quark-meson coupling constant g in Eq. (2·7). We assume that the direct terms in Eq. (2·8) are proportional to the corresponding pieces of the Nijmegen model-F potential.[7] For the S-meson nonet employed in model-F, this can be achieved by replacing $9g^2$ in Eq. (2·10) with

$$9g^2 \rightarrow \begin{cases} c_{\mathcal{P}} f_{a_3 a_1 \beta} f_{a_2 a_4 \beta} & \text{for} \quad \beta = \epsilon, \ S^* \ \text{and} \ \delta \ , \\ c_{\mathcal{P}} f_{a_3 a_2 \kappa} f_{a_1 a_4 \kappa} \ , \end{cases} \tag{2·11}$$

supplemented with appropriate isospin factors. Here $c_{\mathcal{P}}$ denotes the reduction factor which may depend on the flavor symmetry phase $\mathcal{P}$. The values we mainly employ in this paper are the same as in Ref. 15):

$$c_{\mathcal{P}=+1} = 0.56, \qquad c_{\mathcal{P}=-1} = 0.33 \ . \tag{2·12}$$

For the RGM calculation incorporating the non-central forces, the last value is modified into 0.4212, which is the standard value of RGM-F employed in Refs. 16) and 17).

Since we include the MC term and takes account of its contribution to the relative kinetic-energy term, the calculated reduced mass μ_α is only about half of the experimental reduced mass μ_α^{exp}. To use the correct reduced mass is important in the phase shift analysis. For this purpose we employ the prescription given in Ref. 15). The prescription is very simple and does not spoil the Pauli principle in a single-channel problem. What is needed in the prescription is to multiply by $\mu_\alpha / \mu_\alpha^{\text{exp}}$ only the kinetic and MC exchange kernels.

In order to apply the WKB approximation to the RGM equation in Eq. (2·8), we need to simplify the present coupled-channel formulation by neglecting the channel-coupling effect and the non-central forces. The single-channel exchange kernel $G_{\alpha\alpha}(\boldsymbol{R}, \boldsymbol{R}')$ for the $(3q)$-$(3q)$ system is converted to the corresponding Wigner transform through

$$G_{\alpha\alpha}^W(\boldsymbol{R}, \boldsymbol{P}) = \int d\boldsymbol{s} \ e^{\frac{i}{\hbar} \boldsymbol{s} \cdot \boldsymbol{P}} \ G_{\alpha\alpha} \left(\boldsymbol{R} - \frac{\boldsymbol{s}}{2}, \boldsymbol{R} + \frac{\boldsymbol{s}}{2} \right) \ . \tag{2·13}$$

The effective potential, $U_\alpha^{\text{eff}}(R)$, follows from $G_{\alpha\alpha}^W(\boldsymbol{R}, \boldsymbol{P}) \equiv G_{\alpha\alpha}^W(\boldsymbol{R}^2, \boldsymbol{P}^2, (\boldsymbol{R} \cdot \boldsymbol{P})^2)$ by solving the following the transcendental equation

$$U_\alpha^{\text{eff}}(R) = V_{\alpha D}^{CN}(\boldsymbol{R})$$
$$+ G_{\alpha\alpha}^W \left(R^2, 2\mu_\alpha [\varepsilon_\alpha - U_\alpha^{\text{eff}}(R)], 2\mu_\alpha R^2 [\varepsilon_\alpha - U_\alpha^{\text{eff}}(R)] - \hbar^2 \left(L + \frac{1}{2} \right)^2 \right) \ , \tag{2·14}$$

where L is the orbital angular momentum.

§3. Phase shift calculations in RGM

Before showing results of the phase-shift calculation in the RGM, we first discuss the spin-flavor SU_6 symmetry of two octet-baryons in the $S = -2$ sector. Table I

Table I. The relationship between the isospin basis and the flavor-SU_3 basis for the $S = -2$ system. The flavor-SU_3 symmetry is given by the Elliott notation. $\mathcal{P}$ denotes the flavor exchange symmetry, and I the isospin.

	$\mathcal{P} = +1$ (symmetric) ^1E or ^3O	$\mathcal{P} = -1$ (antisymmetric) ^3E or ^1O
$\Lambda\Lambda$	$\frac{1}{\sqrt5}(11)_s + \frac{9}{2\sqrt{30}}(22) + \frac{1}{2\sqrt2}(00)$	–
$\Xi N(I=0)$	$\frac{1}{\sqrt5}(11)_s - \sqrt{\frac{3}{10}}(22) + \frac{1}{\sqrt2}(00)$	$(11)_a$
$\Xi N(I=1)$	$\sqrt{\frac{3}{5}}(11)_s + \sqrt{\frac{2}{5}}(22)$	$\frac{1}{\sqrt3}[-(11)_a + (30) + (03)]$
$\Sigma\Lambda$	$-\sqrt{\frac{2}{5}}(11)_s + \sqrt{\frac{3}{5}}(22)$	$\frac{1}{\sqrt2}[(30) - (03)]$
$\Sigma\Sigma(I=0)$	$\sqrt{\frac{3}{5}}(11)_s - \frac{1}{2\sqrt{10}}(22) - \sqrt{\frac{3}{8}}(00)$	–
$\Sigma\Sigma(I=1)$	–	$\frac{1}{\sqrt6}[2(11)_a + (30) + (03)]$
$\Sigma\Sigma(I=2)$	(22)	–

shows the relationship between the isospin basis and the flavor SU_3 basis for the $S = -2$ system. With regard to the $S = 0$ and -1 systems, see Table I of Ref. 15). As mentioned in the introduction, a comparison of these two tables shows that the flavor singlet (00) state, namely the H-particle, appears only in the $S = -2$ system. It is possible to get some information on those states which have already appeared in the $S = 0$ and -1 systems because the flavor symmetry constrains the interaction in so far as the effect of the FSB is small. For example, we expect that the short-range part of the $\Lambda\Lambda$, $\Sigma\Lambda(\mathcal{P} = +1)$ and $\Sigma\Sigma(I = 2)$ interactions is dominated by the repulsion generated from the color-magnetic interaction, because they have a predominant component of (22) which is nothing but the NN ^1S-state. We also expect that the quark Pauli principle generates the repulsive effect in the $\Xi N(I = 1)$ $(\mathcal{P} = +1)$ and $\Sigma\Sigma(I = 0)$ channels because their main component is $(11)_s$. The most compact $(0s)^6$ configuration of $(11)_s$ symmetry is Pauli forbidden, which is responsible for the strongly repulsive feature of the $\Sigma N(I = 1/2)$ ^1S phase shift.

Next we discuss the role of each term of the Hamiltonian Eq. (2·4) in order to understand qualitative characteristics of the interaction in each channel. The confinement potential U_{ij}^{Cf} does not contribute to the interaction between the baryons in the present approach, as mentioned in Ref. 15). The color-Coulombic potential U_{ij}^{CC} also gives a very minor contribution. On the other hand, both of the exchange contributions from the kinetic energy (K) term and the MC term U_{ij}^{MC} are expected to give a significant contribution to the baryon-baryon interaction. [15] The strength of these terms is approximately (exactly in the SU_3 limit) proportional to the spin-flavor-color factor of the exchange normalization kernel

$$X_N = (-9)\langle \xi_\alpha^{SF}\xi^C | P_{36}^{SFC} | \xi_\alpha^{SF}\xi^C \rangle \ . \tag{3·1}$$

Here P_{36}^{SFC} denotes the exchange operator in the spin-flavor-color space between the third and sixth quarks. The quark Pauli effect represented by the exchange kernels of the K and MC is classified as follows: In a channel with $X_N \sim 0$ the Pauli effect is of course negligible. In the case of $X_N \sim -1$ there exists an almost Pauli-forbidden state in the corresponding S-wave channel, because the smallest eigen-value of the normalization kernel $\mu = 1 + X_N$ becomes close to 0. As the result, the channel tends to get strong repulsion. The Pauli effect generally gives a repulsive contribution when $X_N < 0$, whereas it becomes attractive when $X_N > 0$. The values of X_N in the case of $S = -2$ are listed for each channel in Table II. The values for the S-wave channel are already given in Table 5 of Ref. 21). According to the above discussion, the channels of $S = -2$ can be arranged in decreasing order of the short-range repulsion in the S-wave as follows:

$$\Xi N(I=1)\,^1S > \Sigma\Lambda\,^1S,\,^3S > \Xi N(I=1)\,^3S$$
$$> \Sigma\Sigma(I=0)\,^1S > \Sigma\Sigma(I=1)\,^3S > \Xi N(I=0)\,^3S > \cdots . \quad (3\cdot2)$$

We note that this ordering approximately agrees with that of the size of the corresponding effective hard core radius examined in Ref. 21).

Table II shows that the value of X_N for the ΞN system is determined solely by spin and isospin values, independently of the flavor exchange symmetry $\mathcal{P}$. This suggests that the ΞN interaction is $\mathcal{P}$-independent. This is traced back to the fact that, for the single-quark exchange, the transformation from ΞN ($N\Xi$) to $N\Xi$ (ΞN) is not possible because the FB interaction does not induce the flavor change. On the other hand, two-quark exchange kernels are simply reduced into the single-quark exchange kernels owing to the generalized Pauli principle. Because of this $\mathcal{P}$ independence of the spin-flavor factors, we can expect that the ΞN system has a similar central potential in the ^1S- and ^1P-states and likewise in the ^3S- and ^3P-states. In contrast to the ΞN system, the $\Sigma\Lambda$ system can have the exchange diagram

Table II. The spin-flavor-color factors, X_N, of the exchange normalization kernel for the channel with the flavor exchange symmetry $\mathcal{P}$ and the spin-orbital quantum numbers ^{2S+1}L.

	$\mathcal{P} = +1$		$\mathcal{P} = -1$	
	^1S	^3P	^3S	^1P
$\Lambda\Lambda$	0	$-\frac{2}{3}$	$-$	$-$
$\Xi N(I=0)$	$\frac{1}{3}$	$-\frac{1}{9}$	$-\frac{1}{9}$	$\frac{1}{3}$
$\Xi N(I=1)$	$-\frac{5}{9}$	$-\frac{7}{27}$	$-\frac{7}{27}$	$-\frac{5}{9}$
$\Sigma\Lambda$	$-\frac{1}{3}$	$-\frac{5}{9}$	$-\frac{1}{3}$	-1
$\Sigma\Sigma(I=0)$	$-\frac{2}{9}$	$\frac{8}{27}$	$-$	$-$
$\Sigma\Sigma(I=1)$	$-$	$-$	$-\frac{5}{27}$	$-\frac{1}{9}$
$\Sigma\Sigma(I=2)$	$\frac{1}{9}$	$-\frac{31}{27}$	$-$	$-$

of $\Sigma\Lambda \to \Lambda\Sigma$ through an operator with $I = 1$, e.g., the δ-meson exchange. Indeed we find that X_N in the $\Sigma\Lambda$ system is $\mathcal{P}$-dependent.

The contribution from the color-magnetic (GC) term U_{ij}^{GC} is discussed next. It is known that the spin-spin term in Eq. (2·6) yields strong attraction in the H-particle channel[4] of the flavor-singlet (00) symmetry;

$$(00) = \frac{1}{\sqrt{8}} \Lambda\Lambda + \frac{2}{\sqrt{8}} \Xi N - \sqrt{\frac{3}{8}} \Sigma\Sigma \ . \qquad (3·3)$$

If the effect of the FSB is neglected ($m_s = m_{ud} = m$), it is possible to estimate the contribution of the GC term to each of the $\Lambda\Lambda$, $\Xi N(I = 0)$ and $\Sigma\Sigma(I = 0)$ channels, by employing a simple formula given in Refs. 4) and 11). We consider the energy difference between $(0s)^6$ and two-$(0s)^3$ configurations. The expectation value of the GC term for the totally antisymmetric $(0s)^n$ quark states is given, in units of $\sqrt{2/\pi}\alpha_S(\hbar/mcb)^3 mc^2(1/16)$, by

$$\langle -\sum_{i>j}^{n}(\lambda_i^c \cdot \lambda_j^c)\left(1 + \frac{2}{3}\boldsymbol{\sigma}_i \cdot \boldsymbol{\sigma}_j\right)\rangle = \frac{2}{3}\langle C_2\rangle_{(\lambda\mu)} + \frac{8}{9}S(S+1) + \frac{2}{3}n(n-6) \ , \quad (3·4)$$

where C_2 is the Casimir operator for flavor-SU_3 group and its expectation value is given by

$$\langle C_2\rangle_{(\lambda\mu)} = \frac{4}{3}(\lambda^2 + \mu^2 + \lambda\mu + 3\lambda + 3\mu) \qquad (3·5)$$

for a state of the flavor SU_3 symmetry $(\lambda\mu)$. The difference between the $(0s)^6$ and $2 \times (0s)^3$ configurations is $-16/3$ for the H-particle state, while it becomes $32/3$, 0 and $-32/7$ in the ^1S states of $\Lambda\Lambda$, $\Xi N(I = 0)$ and $\Sigma\Sigma(I = 0)$, respectively. We expect that the $\Lambda\Lambda$ interaction generated from the GC term shows the repulsive behavior at the short distance. In the other channels than the three discussed here, the characteristic behavior of the interaction is generally determined by the $K + MC$ term rather than by the GC term.

Table III. The quark-model parameters, the scalar-meson masses, and the SU_3 parameters of the effective meson-exchange potential. The symbol f_1 (f_8) denotes the flavor-singlet (flavor-octet) coupling constant, α the $F/(F + D)$ ratio, and θ the singlet-octet mixing angle. The ϵ mass denoted by "two-pole" indicates two-pole approximation, for which $m_1 c^2$ (β_1) and $m_2 c^2$ (β_2) are shown below the table. For c_P, see text.

b (fm)	$m_{ud}c^2$ (MeV)	α_S	$\lambda = m_s/m_{ud}$
0.6	313	1.5187	1.25
$m_\epsilon c^2$ (MeV)	$m_{S^*}c^2$ (MeV)	$m_\delta c^2$ (MeV)	$m_\kappa c^2$ (MeV)
two-pole*	1250	1255	1245
f_1	f_8	α	θ (degrees)
4.30881	0.93649	1.49640	37.6964

*508.52 MeV (0.19986) and 1043.79 MeV (0.55241)[6]

Table III lists the parameter set used in the present paper.[15] The QM parameters are set to satisfy the single baryon properties as usual, while the EMEP parameters are taken from the Nijmegen model-F[7] without any alteration.

In what follows we display the phase shifts obtained by solving the RGM equation of Eq. (2·8) decomposed into partial waves. Only the central component of the interaction is included in the calculation. The phase-shift curves of the $\Lambda\Lambda$, $\Xi N(I = 0)$ and $\Sigma\Sigma(I = 0)$ channels are shown in Figs. 1(a) (S-waves) and 1(b) (P-waves). It is clear from Fig. 1(a) that a bound state exists in the $\Xi N\,{}^{1}S$ and $\Sigma\Sigma\,{}^{1}S$ states. The binding energy is 9.65 MeV from the ΞN threshold and 42.62 MeV from the $\Sigma\Sigma$ threshold, respectively. These bound states are realized through the attractive nature of the $K + MC$ term for the $\Xi N\,{}^{1}S$ state and of the GC term for the $\Sigma\Sigma\,{}^{1}S$ state, in addition to the moderate flavor dependence of the overall attraction from the EMEP's. Our result indicates that the $\Xi N\,{}^{3}S$ state has no bound state, in contrast to the result of Ref. 13). This channel does not couple to any other two-baryon channels. The

Fig. 1. The $\Lambda\Lambda$, $\Xi N(I = 0)$ and $\Sigma\Sigma(I = 0)$ phase shifts predicted by the central force of the present model under the single-channel approximation: (a) the S-wave, (b) the P-wave. The momentum in the laboratory system, p_{lab}, stands for the momentum of particle B_1 for $B_1 B_2$ system.

$\Xi N\,{}^{3}S_1$ phase shift is raised up to 18 degrees when the tensor force is turned on. The central potential of the $\Xi N(I = 0)\,{}^{3}S$ state is less attractive than the ${}^{1}S$ state because of the flavor dependence of the EMEP through Eq. (2·12), in addition to the repulsive nature of the GC term. The $\Lambda\Lambda\,{}^{1}S$ phase shift is similar to the NN S wave phase shift through the behavior of the GC term, and it is fairly close to that of Ref. 12). The strong attraction in the $\Sigma\Sigma\,{}^{3}P$ state is due to the attractive behavior of the $K + MC$ term as suggested from the large X_N value in Table II. The $\Xi N\,{}^{1}P$ and $\Xi N\,{}^{3}P$ phase shifts are very similar. This is due to the fact that the potentials of both channels have almost same attraction in the long range region. As seen in the next section, the attraction of the $\Xi N\,{}^{1}P$ channel is, however, stronger than that of the $\Xi N\,{}^{3}P$ channel in the region of less than 1.5 fm.

The phase shift curves of the $\Xi N(I = 1)$, $\Sigma\Lambda$ and $\Sigma\Sigma(I = 1)$ channels are shown in Figs. 2(a) (S-waves) and 2(b) (P-waves). All the channels in Fig. 2(a) have negative phase shifts. These are due to the repulsive behavior of the $K + MC$
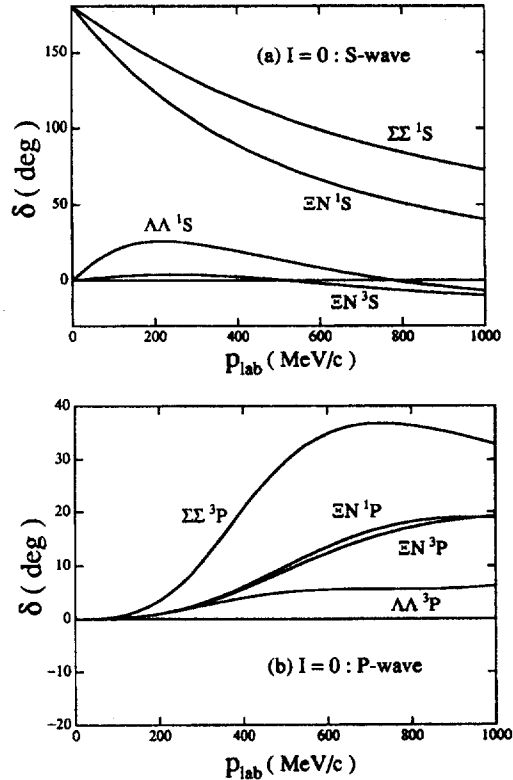
term as all the X_N values are negative. Although the X_N values of all the channels in Fig. 2(b) are also negative, the phase shifts in the $\Xi N\,{}^3P$, $\Sigma\Lambda\,{}^3P$ and $\Sigma\Sigma\,{}^1P$ states are slightly attractive, because the EMEP's produce weak attraction in the tail region.

We show the phase shift for the $I = 2$ channel in Fig. 3. The phase shift in the $\Sigma\Sigma\,{}^1S$ state with pure (22) symmetry is similar to that in the $NN\,{}^1S$ state. The phase shift of the $\Sigma\Sigma\,{}^3P$ channel is repulsive due to the repulsive Pauli effect ($X_N = -31/27$).

A short remark follows as to the FSB. The FSB generated from the mass difference between ud and s quarks is explicitly incorporated in the present calculation through the Hamiltonian Eq. (2·4). The effect is expected to be more significant in the $S = -2$ system than in the $S = -1$ system. To see this we have changed λ from 1.25 to 1.69.[20] Although the change of the phase shifts is strongly channel dependent, it is larger as the energy increases, and is certainly larger than that in the $S = -1$ case. Those channels which

Fig. 2. The same as Fig. 1, but for the $\Xi N(I = 1)$, $\Sigma\Lambda$ and $\Sigma\Sigma(I = 1)$ phase shifts.

have the strongest λ dependence are the $\Sigma\Lambda\,{}^1S$, $\Sigma\Sigma(I = 0)\,{}^3P$, $\Sigma\Sigma(I = 1)\,{}^3S$ and $\Sigma\Sigma(I = 2)\,{}^1S$ states, where the maximum change of the phase shift reaches about 12 degrees. The channels of the $\Sigma\Lambda\,{}^3S$, $\Lambda\Lambda\,{}^1S$, ${}^3P$, $\Sigma\Sigma(I = 0)\,{}^1S$ and $\Sigma\Sigma(I = 1)\,{}^1P$ states have the change of at most 6 degrees. The ΞN channel shows relatively small λ-dependence. As to the H-particle channels, increasing λ yields more attractive behavior in $\Lambda\Lambda$ and $\Sigma\Sigma$ channels and more repulsive behavior in ΞN channel, respectively.

To estimate the cross sections induced by the $\Xi^- p$ reaction, we now solve the coupled-channel equation, Eq. (2·8), by including the non-central components due to the FB interaction and the tensor component due to the π- and K-exchanges. The value of $c_{\mathcal{P}=-1}$ in Eq. (2·12) is altered to $c_{\mathcal{P}=-1} = 0.4212$, in order to be consistent with the NN data as discussed in Refs. 16) and 17). The present calculation includes the partial waves up to the total angular momentum $J = 3$ and incorporates the Coulomb force approximately. The single-channel calculation without the ΞN - $\Lambda\Lambda$ coupling predicts the following cross sections at $p_\Xi = 500$ MeV/c: $\sigma_{\rm el}(\Xi^- p) = 31.1$ mb and $\sigma(\Xi^- p \to \Xi^0 n) = 32.4$ mb. They decrease to 27.7 and 28.4 mb at 600 MeV/c, respectively. The near equality of both cross sections is understood by the
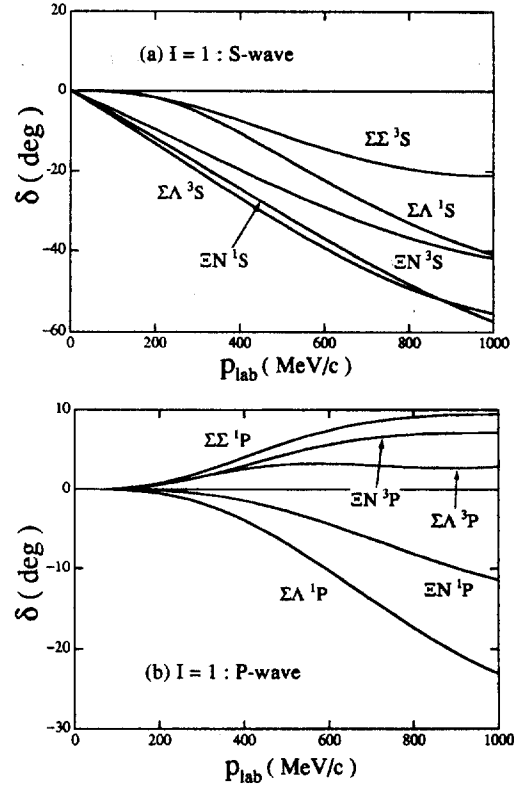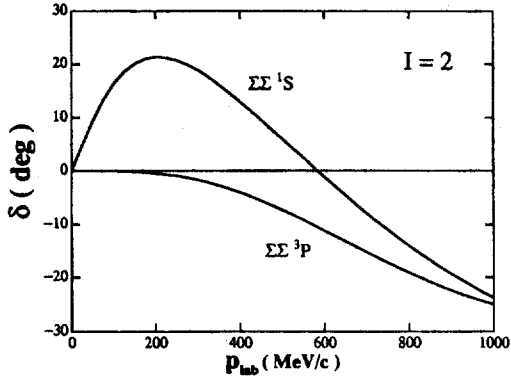
Fig. 3. The same as Fig. 1, but for the $\Sigma\Sigma(I = 2)$ phase shifts.

fact that the ΞN potential with $I = 1$ channel is repulsive and thus gives a minor contribution to the cross sections. When the ΞN - $\Lambda\Lambda$ coupling is turned on, the above cross sections decrease a little: $\sigma_{\mathrm{el}}(\Xi^- p) = 27.7$ mb and $\sigma(\Xi^- p \to \Xi^0 n) = 24.5$ mb at 500 MeV/c. The reaction cross section $\sigma(\Xi^- p \to \Lambda\Lambda)$ becomes 15.4 mb. If we compare these results with predictions by $S = -2$ Nijmegen hard-core models which assume the hard-core radii of the NN system, [22] the elastic cross sections are similar to each other whereas our reaction cross sections are larger than those of the Nijmegen models.

We next estimate the energy of the H-particle state by including the three channels of $\Lambda\Lambda, \Xi N(I = 0)$ and $\Sigma\Sigma(I = 0)$. Only the central force plays a role in this system. The energy for a pure $(0s)^6$ configuration becomes 72 MeV above the $\Lambda\Lambda$ threshold, whereas it goes down to -19.25 MeV when the relative motion between the two baryons is dynamically solved by the variational principle. We should note that this value may be overestimated because the present model produces the threshold energies for $\Xi N - \Lambda\Lambda$ and $\Sigma\Sigma - \Lambda\Lambda$ too low; i.e., they are 19.8 MeV and 78.2 MeV corresponding to the experimental values 25.7 MeV and 154.9 MeV, respectively. The improvement of these threshold energies may reduce the present value of the binding energy.

§4. Behavior of the effective local potentials

In this section, we investigate the effective local potential obtained by solving the transcendental equation of Eq. (2·14), in order to understand intuitively the baryon-baryon interaction in the $S = -2$ sector. It sometimes happens, however, that a real solution cannot be obtained when the repulsion due to the effect of the Pauli principle is too strong. [15] In this case we define the effective local potential by employing the incident momentum for the local momentum. The obtained effective local potential is still useful for understanding the baryon-baryon interaction at least qualitatively, though it may be no longer "equivalent". We also note that, even when the transcendental equation has a real solution, the phase shift calculated by the effective potential sometimes deviates by about 10 degrees from the original RGM phase shift in the case that the Pauli effect is fairly large. All the effective local potentials shown here correspond to the zero incident energy.

Figure 4 shows the ^1S potentials of the $\Lambda\Lambda$, $\Xi N(I = 0)$ and $\Sigma\Sigma(I = 0)$ channels which constitute the H-particle. The total potential has different characteristics in each channel: It is similar to the NN S-wave potential in the $\Lambda\Lambda$ channel, has broad attraction in the ΞN channel, and has deep attraction in the $\Sigma\Sigma$ channel.
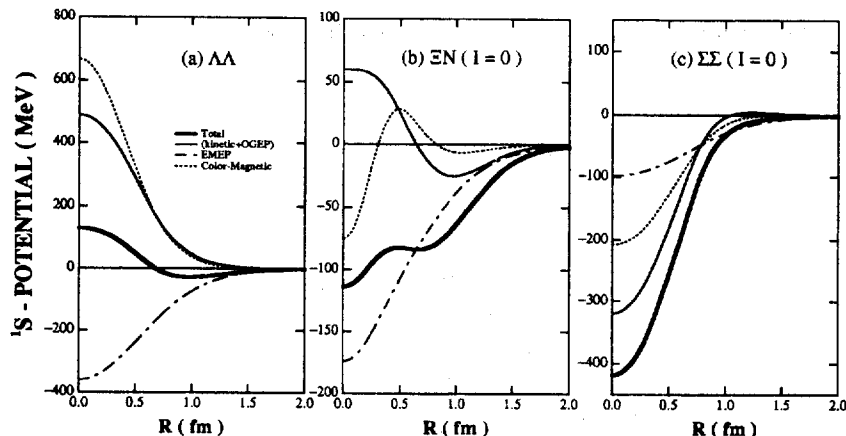
Fig. 4. The ^1S-potentials of the (a) $\Lambda\Lambda$, (b) $\Xi N(I = 0)$ and (c) $\Sigma\Sigma(I = 0)$ channels, where the total potential (bold curve) is shown together with the contributions from the (kinetic + OGEP)-term (solid curve), the effective meson-exchange potential (dot-dashed curve) and the color-magnetic (GC) term (dotted curve).

The qualitative behavior of the (kinetic+OGEP) curves agrees with that given in Ref. 10). The GC (color magnetic) contribution is consistent with the expectation given by Eq. (3·4). In particular it has the short range repulsion in the $\Lambda\Lambda\,^1S$ state. The $K + MC$ contribution in the $\Xi N\,^1S$ state shows the strong attractive behavior at the medium-range due to the positive value of $X_N = 1/3$. The attraction in the $\Sigma\Sigma\,^1S$ channel is largely due to the GC term which enhances the weak attraction of the EMEP.

We show in Fig. 5 the ΞN potentials for most important channels of the $\Xi^- p$ scattering; (a) $I = 0$, spin-singlet, (b) $I = 0$, spin-triplet, (c) $I = 1$, spin-singlet and (d) $I = 1$, spin-triplet. As discussed in §2, the P-wave potential is similar to the S-wave potential with the same spin and isospin values, except for the extremely short-ranged region of $R < 0.5$ fm. The QM predicts that the ΞN potential is attractive in the $I = 0$ channel but repulsive in the $I = 1$ channel. This isospin dependence is different
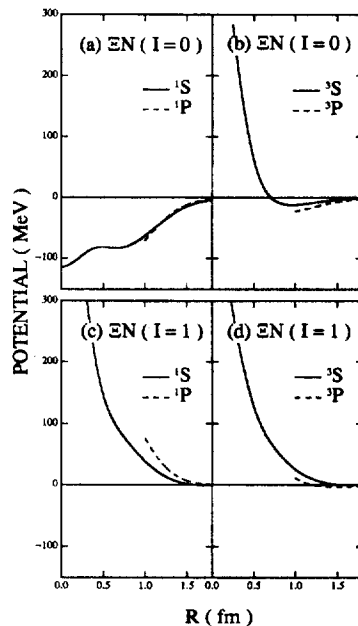

Fig. 5. The ΞN central potentials for (a) the spin-singlet state of the $I = 0$ channel, (b) the spin-triplet state of the $I = 0$ channel, (c) the spin-singlet state of the $I = 1$ channel and (d) the spin-triplet state of the $I = 1$ channel. The solid curve stands for the S-wave potential and the dashed curve for the P-wave one.

from that of the Nijmegen hard core potential as discussed later.

The $\Lambda\Lambda^3P$ potential shown in Fig. 6 is repulsive because of the $K + MC$ contribution. The slight attraction appearing in the region of more than 1.5 fm, however, makes the phase shift positive as seen in Fig. 1(b).

We compare the present QM potential with the Nijmegen potential in Table IV which lists the qualitative behavior of the potentials in the medium range of $0.6 - 1.2$ fm for each channel. The Nijmegen model-D and model-F potentials give different behavior in ten channels among twenty channels. There are two reasons for this difference. First, the contribution from the S-meson exchange is different between the model-D and model-F:[1],[2] Only the flavor singlet S-meson exchange is introduced in the model-D, leading to the YN and YY potentials which are as attractive as the NN potential. On the other hand, the S-meson nonet exchange is used in the model-F and naturally produces the flavor dependent attraction in the medium range of the YN or YY potentials. The difference in the $\Lambda\Lambda$ and $\Sigma\Lambda$ systems is understood by this reason. Secondly, the spin-spin interaction generated from the vector- (V-
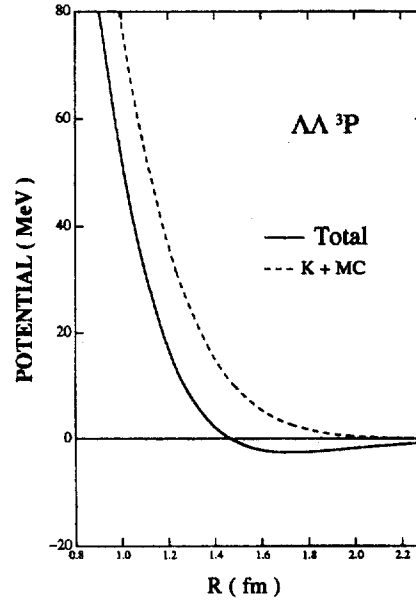

Fig. 6. The $\Lambda\Lambda^3P$ central potential. The solid curve stands for the total potential and the dashed curve the contribution from the kinetic (K) and momentum-dependent retardation (MC) terms.

Table IV. A characteristic behavior of the Nijmegen model-D (D), model-F (F) and quark model (QM) central potentials at the distance of 0.6 - 1.2 fm. The symbol a means the attractive behavior and r the repulsive one.

	^1S			^3P			^3S			^1P		
	D	F	QM	D	F	QM	D	F	QM	D	F	QM
$\Lambda\Lambda$	a	a	a	a	r	r		—			—	
$\Xi N(I=0)$	a	r	a	a	a	a	a	a	a	a	r	a
$\Xi N(I=1)$	a	r	r	a	a	r	a	a	r	a	r	r
$\Sigma\Lambda$	a	a	r	a	r	r	a	r	r	a	r	r
$\Sigma\Sigma(I=0)$	a	r	a	a	a	a		—			—	
$\Sigma\Sigma(I=1)$		—			—		a	a	r	a	r	r
$\Sigma\Sigma(I=2)$	a	a	a	r	r	r		—			—	

) meson exchange has different behavior between these two models: It is repulsive in the model-D but attractive in the model-F. As a result the central force in the spin-singlet state becomes attractive in the model-D and repulsive in the model-F. This mechanism explains the difference in the ΞN and $\Sigma\Sigma$ systems.

Among the ten channels where the model-D and model-F give similar behavior, the QM predicts different results, namely the repulsive potentials in the four channels, $\Xi N(I=1)\,^3S$, $\Xi N(I=1)\,^3P$, $\Sigma\Lambda\,^1S$ and $\Sigma\Sigma(I=1)\,^3S$. These channels are characterized by the repulsion due to the $K+MC$ term as they have $X_N \sim -\frac{1}{3}$. All the potentials become attractive in the other channels except for the $\Sigma\Sigma\,(I=2)\,^3P$ channel. As for another group of the ten channels where the model-D potential is attractive and the model-F potential is repulsive, the QM predicts mostly the repulsive behavior. In fact the potentials of the channels $\Lambda\Lambda\,^3P$, $\Xi N\,(I=1)\,^1S$ and ^1P, $\Sigma\Lambda\,^3P$, ^3S and ^1P, and $\Sigma\Sigma(I=1)\,^1P$ become repulsive due to the repulsive contribution of the $K+MC$ term. However, the QM gives attraction in the remaining three channels of $\Xi N\,(I=0)\,^1S$, ^1P and $\Sigma\Sigma\,(I=0)\,^1S$ in agreement with the model-D. The $K+MC$ term plays an important role to produce attraction in the $\Xi N(I=0)$ channel as understood by $X_N = \frac{1}{3}$, while the GC term becomes important in the $\Sigma\Sigma$ channel as is already discussed below Eq. (3.5).

Figure 7 compares the QM potentials to the Nijmegen hard core potentials for the $^1S(I=0)$ channels of $\Lambda\Lambda$, ΞN and $\Sigma\Sigma$. The QM potentials are found to follow the model-D potentials qualitatively. It is interesting that, though the present QM constructs the EMEP employing the S-meson parameters of the model-F rather than the model-D, the resulting $^1S(I=0)$ potential is similar to the model-D in the channels comprising the H-particle. This originates from the behavior of the spin-spin interaction as discussed above. The spin-spin potential, which is enhanced by a
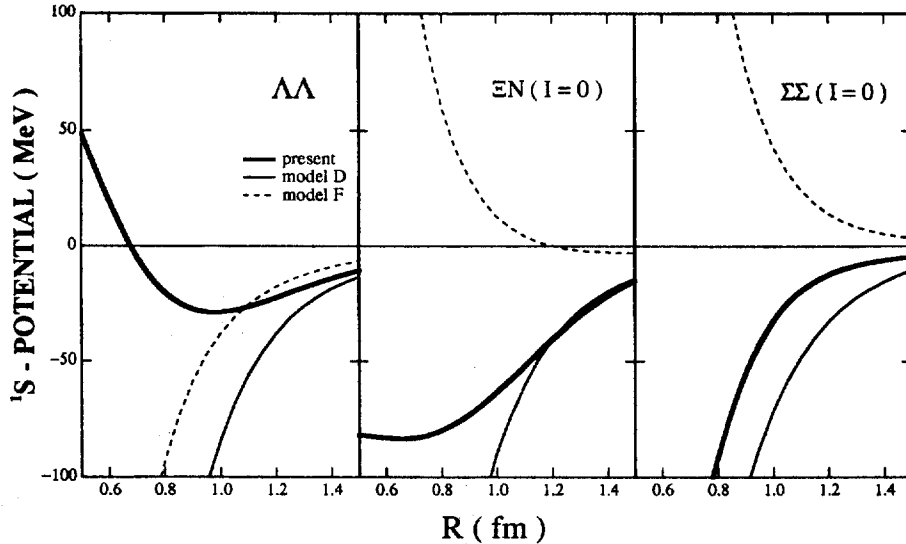

Fig. 7. The comparison of the ^1S-potentials between the present model (bold curve) and the Nijmegen hard-core potentials, the model-D (solid curve) and model-F (dashed curve).

factor of -3 in the $^1S(I = 0)$ channel, comes mainly from the V-meson exchange in the Nijmegen model. It is repulsive in the model-D but attractive in the model-F. The spin-spin potential of the QM is, however, given only by the quark part of the Hamiltonian and turns out to be qualitatively similar to the model-D.

We summarize the QM prediction for the ΞN potential since it is crucial to the $\Xi^- p$ cross sections. The ^1S ($I = 0$) potential is attractive in agreement with the model-D. The ^3S ($I = 0$) potential shows weak attraction of about -20 MeV in the medium-range region as seen in Fig. 5(b), which agrees with both the model-D and model-F. We may conclude that the ΞN potential is attractive in the $I = 0$ channel. The ^1S ($I = 1$) potential is repulsive in the QM as well as in the model-F. The ^3S ($I = 1$) potential is also repulsive in the QM, while it is attractive in both of the model-D and model-F though the depth of the attraction in the model-F is only one third of that in the model-D. The ΞN potential in the $I = 1$ channel is repulsive in the QM, weakly repulsive in the model-F and attractive in the model-D. It is interesting to investigate how this difference of model predictions affects the $\Xi^- p$ cross sections.
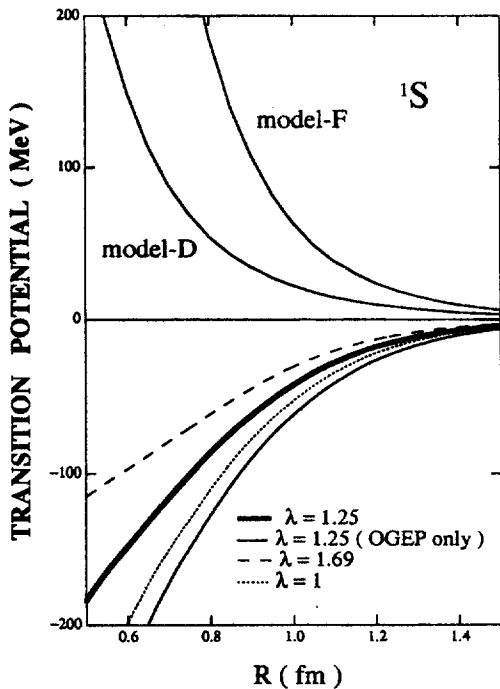

Fig. 8. The comparison of the ΞN - $\Lambda\Lambda$ transition potentials for the ^1S state between the present model and the Nijmegen hard-core models. The transition potential of the present model is given by the $P = 0$ Wigner transform at the ΞN incident channel. Also shown is the dependence of the transition potential on the mass ratio $\lambda = m_s/m_{ud}$.

Finally a comment follows as to the channel-coupling effect. In order to estimate the qualitative feature of the ΞN-$\Lambda\Lambda$ coupling effect in the S-wave, we calculate the $P = 0$ Wigner transform for the transition potential from ΞN to $\Lambda\Lambda$. Figure 8 shows the obtained transition potential, together with the corresponding Nijmegen potential. Only the strange-meson exchange contributes to this ΞN-$\Lambda\Lambda$ transition potential in the Nijmegen model, and it is larger in the model-F than in the model-D [23] as seen in Fig. 8. In the QM term the ΞN-$\Lambda\Lambda$ transition potential of the ^1S-channel is generated only from the κ-meson exchange and the GC term. The ΞN-$\Lambda\Lambda$ transition potential of the QM differs in its sign from that of the Nijmegen model. To see the effect of the FSB on the coupling effect, the transition potential is drawn as a function of λ in Fig. 8. The transition potential is smaller as the FSB becomes larger and the strength of the transition potential with $\lambda = 1$ is about twice larger than that with $\lambda = 1.69$. The reason for this is that the GC term is smaller as the effect of the FSB becomes larger. This

feature is suggested in Ref. 24), which reports that the RGM calculation with only the OGEP for the H-particle state gives a bound state with the binding energy of -38 MeV in the flavor SU_3 limit but no bound state when introducing the FSB with about $\lambda = 1.67$. The difference between bold and solid curves in Fig. 8 comes from the contribution of the κ-meson and it reduces the contribution from the GC term.

§5. Summary

Motivated by the planned $\Xi^- p$ scattering experiment, we have studied the central force of the two-baryon systems with the strangeness $S = -2$. As a natural extension of our previous work on the $S = 0$ and -1 systems, we have adopted the resonating-group (RGM) formulation of the $(3q)$-$(3q)$ system in the SU_6 quark model. The qq interaction includes the central force generated from the scalar-meson nonet exchanges and the tensor force generated from the π- and K-meson exchanges, in addition to the phenomenological confinement potential and a one-gluon exchange potential (OGEP) with explicit quark-mass dependence. This model, which we call RGM-F, gives a realistic description of the NN, ΛN and ΣN interactions, and can straightforwardly be extended to the $S = -2$ sector.

The effect of the quark Pauli principle manifests itself most clearly through the behavior of the kinetic-energy exchange term and the momentum-dependent retardation term. This behavior characterizes the innermost central part of the baryon-baryon interaction in the $S = -2$ systems similarly to the $S = 0$ and -1 systems. An exception is the ^1S state in the $I = 0$ channel of the $\Lambda\Lambda$, ΞN and $\Sigma\Sigma$ systems (H-particle channels), where the color-magnetic term plays a dominant role. The S- and P-wave phase-shifts of all the systems with $S = -2$ are calculated in a single-channel RGM approximation. It appears that the interaction in the $S = -2$ system as a whole is attractive in the $I = 0$ channels but repulsive in the $I = 1$ channels. Our phase shifts of the $\Lambda\Lambda\ ^1S$ and $\Sigma\Sigma(I = 2)\ ^1S$ channels are similar to those of Refs. 12) and 13), respectively. Two bound states are obtained in the H-particle channels: one for the $\Xi N(I = 0)\ ^1S$ channel and the other for the $\Sigma\Sigma(I = 0)\ ^1S$ channel. The former gets attraction from the effect of the Pauli principle, while the latter is due to the color-magnetic interaction. We have found a single bound state of -19.25 MeV below the $\Lambda\Lambda$ threshold, when the three channels, $\Lambda\Lambda$, ΞN and $\Sigma\Sigma$, are coupled together in the coupled-channel RGM formalism. Our calculation has predicted no bound state in the $\Xi N(I = 0)\ ^3S$ channel.

The effective local potential arising from the present quark model is calculated under the WKB approximation. Although the color-magnetic term is not always responsible for the attraction, the full potential for each H-particle channel is attractive as a whole. The ΞN potential is found to be independent of the flavor exchange symmetry, but depends on the isospin: it is attractive in the $I = 0$ channel and repulsive in the $I = 1$ channel. Our quark-model potential is compared with the Nijmegen model-D and model-F potentials. The quark-model potential is qualitatively close to the model-F potential in the medium region when the Pauli effect plays a repulsive role, but is rather close to the model-D potential if the model-D and model-F give a different feature for the spin-spin interaction of the vector-meson

exchange.

The effect of the flavor symmetry breaking is expected to be important for a quantitative analysis of the binding energy of the H-particle and the Ξ^-p cross sections. The effect is investigated in the present model by varying the mass ratio of the up-down and strange quarks, $\lambda = m_s/m_{ud}$. It strongly depends on the channel and is larger than that in the $S = -1$ case. For example, the binding energy of the H-particle is increased from 19.25 MeV to 64.21 MeV, if $\lambda = 1.25$ is modified into $\lambda = 1$. An estimate of the ΞN-$\Lambda\Lambda$ transition potential clearly shows that the effect of the flavor symmetry breaking reduces the coupling effect between these two channels.

The Ξ^-p total cross sections are calculated in the coupled-channel RGM formalism for the ΞN - $\Lambda\Lambda$ system. The Coulomb force is approximately treated and the isospin relation is employed to generate the scattering amplitudes in the particle basis. At $p_\Xi = 500$ MeV/c these total cross sections are given by 27.7 mb for the Ξ^-p elastic scattering, 24.5 mb for the $\Xi^-p \rightarrow \Xi^0n$ charge-exchange reaction, and 15.4 mb for $\Xi^-p \rightarrow \Lambda\Lambda$ reaction. This value for the Ξ^-p elastic cross section is very similar to the result by $S = -2$ Nijmegen hard-core models which assume the same hard-core radii as in the NN system. On the other hand, our $\Xi^-p \rightarrow \Lambda\Lambda$ reaction cross section is considerably larger than that of the Nijmegen models.

The data of the double-Λ hypernuclei obtained so far and the old emulsion data of the Ξ hypernuclei seem to require considerable attraction in both of the ΞN and $\Lambda\Lambda$ channels. This favors the Nijmegen model-D rather than the Nijmegen model-F.[3] The present quark model predicts, however, that the ΞN interaction is strongly channel dependent, and is not as strongly attractive as the model-D. Especially the quark-model potential for the ΞN interaction is strongly repulsive in the $I = 1$ channel. It will be important to examine if our result is consistent with the above-mentioned hypernucleus data. Predictions of the H-particle binding energy and the ΞN cross sections in terms of the other versions of our quark model, FSS [18),19)] and RGM-H [19)], should also be examined.

Acknowledgements

References

1) C. B. Dover and A. Gal, Prog. Part. Nucl. Phys. **12** (1984), 171.
2) Yasuo Yamamoto and Hiroharu Bandō, Prog. Theor. Phys. Suppl. No.81 (1985), 9.
3) Yasuo Yamamoto, Toshio Motoba, Hiroyuki Himeno, Kiyomi Ikeda and Shinobu Nagata, Prog. Theor. Phys. Suppl. No. 117 (1994). 361.
4) R. L. Jaffe, Phys. Rev. Lett. **38** (1977), 195.
5) S. Aoki *et al.*, Prog. Theor. Phys. **85** (1991), 1287.
6) M. M. Nagels, T. A. Rijken and J. J. de Swart, Phys. Rev. **D12** (1975), 744; **15** (1977),

2547.
7) M. M. Nagels, T. A. Rijken and J. J. de Swart, Phys. Rev. **D20** (1979), 1633.
8) M. M. Nagels, T. A. Rijken and J. J. de Swart, Phys. Rev. **D17** (1978), 768.
    M. Maessen, Th. A. Rijken and J. J. de Swart, Phys. Rev. **C40** (1989), 2226.
9) B. Holzenkamp, K. Holinde and J. Speth, Nucl. Phys. **A500** (1989), 485.
    A. Reuber, K. Holinde and J. Speth, Nucl. Phys. **A570** (1994), 543.
10) M. Oka and K. Yazaki, in *Quarks and Nuclei*, ed. W. Weise (World Scientific, Singapore, 1984), p. 489.
11) Kiyotaka Shimizu, Rep. Prog. Phys. **52** (1989), 1.
12) U. Straub, Zong-Ye Zhang, K. Bräuer, Amand Faessler and S. B. Khadkikar, Phys. Lett. **B200** (1988), 241.
13) Y. Koike, K. Shimizu and K. Yazaki, Nucl. Phys. **A513** (1990), 653.
14) Sachiko Takeuchi and Makoto Oka, Phys. Rev. Lett. **66** (1991), 1271.
15) C. Nakamoto, Y. Suzuki and Y. Fujiwara, Prog. Theor. Phys. **94** (1995), 65.
16) Y. Fujiwara, C. Nakamoto and Y. Suzuki, Prog. Theor. Phys. **94** (1995), 215.
17) Y. Fujiwara, C. Nakamoto and Y. Suzuki, Prog. Theor. Phys. **94** (1995), 353.
18) Y. Fujiwara, C. Nakamoto and Y. Suzuki, Phys. Rev. Lett. **76** (1996), 2242.
19) Y. Fujiwara, C. Nakamoto and Y. Suzuki, Phys. Rev. **C54** (1996), 2180.
20) C. Nakamoto, Y. Suzuki and Y. Fujiwara, Pys. Lett. **B318** (1933), 587.
21) M. Oka, K. Shimizu and K. Yazaki, Nucl. Phys. **A464** (1987), 700.
22) Yasuo Yamamoto, private communication.
23) Yasuo Yamamoto, Hideo Takaki and Kiyomi Ikeda, Prog. Theor. Phys. **86** (1991), 867.
24) M. Oka, K. Shimizu and K. Yazaki, Phys. Lett. **B130** (1983), 365.